University of Nebraska - Lincoln Digital Commons@University of Nebraska - Lincoln

Christian Binek Publications

Research Papers in Physics and Astronomy

11-15-1994

Interface alloying and magnetic properties of Fe/ Rh multilayers

K. Hanisch

Laboratorium fir Angewandte Physik, Universitat Duisburg, Germany

W. Keune

Laboratorium fir Angewandte Physik, Universitat Duisburg, Germany

R.A. Brand

Laboratorium fir Angewandte Physik, Universitat Duisburg, Germany

Christian Binek

University of Nebraska-Lincoln, cbinek2@unl.edu

W. Kleeman

Laboratorium fir Angewandte Physik, Universitat Duisburg, Germany

Follow this and additional works at: http://digitalcommons.unl.edu/physicsbinek



Part of the Physics Commons

Hanisch, K.; Keune, W.; Brand, R.A.; Binek, Christian; and Kleeman, W., "Interface alloying and magnetic properties of Fe/Rh multilayers" (1994). Christian Binek Publications. Paper 4. http://digitalcommons.unl.edu/physicsbinek/4

This Article is brought to you for free and open access by the Research Papers in Physics and Astronomy at Digital Commons@University of Nebraska-Lincoln. It has been accepted for inclusion in Christian Binek Publications by an authorized administrator of DigitalCommons@University of Nebraska - Lincoln.

Interface alloying and magnetic properties of Fe/Rh multilayers

K. Hanisch, W. Keune, R. A. Brand, C. Binek, and W. Kleemann Laboratorium für Angewandte Physik, Universität Duisburg, D-47048 Duisburg, Germany

Rh(20 Å)/ 57 Fe($t_{\rm Fe}$) multilayers with Fe thicknesses $t_{\rm Fe}$ of 2, 5, 10, and 15 Å prepared by alternate evaporation in UHV have been investigated by x-ray diffraction (XRD), Mössbauer spectroscopy, and SQUID magnetometry. First- and second-order superstructure Bragg peaks (but no higher-order peaks) in small-angle XRD patterns suggest some compositional modulation. Mössbauer spectra taken at 4.2 K are characterized by a distribution $P(B_{\rm hf})$ of hyperfine fields $B_{\rm hf}$. Peaks observed in the $P(B_{\rm hf})$ curves near 17 and 35 T are assigned to an fcc-RhFe interface alloy (~7-24 at. % Fe) with spin-glasslike properties and to a disordered ferromagnetic bcc-FeRh alloy (~96 at. % Fe), respectively. The magnetic transition temperature of the fcc alloy was found to be 23 and 45 K for $t_{\rm Fe}$ =2 and 5 Å, respectively, and $B_{\rm hf}$ follows a $T^{3/2}$ law. For $t_{\rm Fe}$ =2 Å, spin-glasslike behavior was observed by magnetometry.

Metallic multilayered films offer an exciting field for the exploration of magnetic properties in novel systems and at interfaces.¹ In a search for new multilayers with interesting magnetic behavior we have studied the Fe-Rh system. According to the thermodynamic Fe-Rh phase diagram² a wide solubility range exists at rather low temperatures on both the Fe-rich and Rh-rich side. Therefore, a tendency for interfacealloy formation may be expected in these multilayers. The properties of Fe/Rh interfaces are unknown so far.

We have prepared a series of Rh/Fe multilayers with constant Rh thickness (20 Å) by alternating evaporation of Rh and ⁵⁷Fe isotope (95% enriched) in an UHV system. The pressure during evaporation was <5×10⁻⁹ mbar. The substrates were polyimid foils for Mössbauer and magnetometric studies and Si wafers for small- and large-angle x-ray diffraction (XRD). To reduce intermixing, the substrate temperature was held at ~100 K during multilayer growth. Rh and ⁵⁷Fe were evaporated from a 2-kW electron-beam gun and a small resistively heated evaporation cell with alumina crucible, respectively. Four different types of multilayers have been prepared, namely [Rh(20 Å)/⁵⁷Fe(2 Å)]₁₀₀+Rh(20 Å), [Rh(20 Å)/⁵⁷Fe(5 Å)]₅₂+Rh(20 Å), [Rh(20 Å)/⁵⁷Fe(10 Å)]₃₀+Rh(20 Å), and [Rh(20 Å)/Fe(15 Å)]₂₀+Rh(20 Å). (All samples were coated by 20 Å Rh for protection.)

The small-angle XRD patterns (Fig. 1) exhibit a clear first-order superstructure Bragg peak for all samples, and an additional second-order peak for $t_{\rm Fe}$ =10 and 15 Å. This and the fact that no higher-order superstructure peaks have been detected (not shown in Fig. 1) demonstrates qualitatively that our samples are compositionally modulated structures with some degree of intermixing at the interfaces. The multilayer periodicity determined from Fig. 1 is 23.7, 24.9, 29.7, and 37.7 Å for $t_{\rm Fe}$ =2, 5, 10, and 15 Å, respectively, being in agreement with the nominal periodicity within 7% or better. The large-angle XRD patterns from our samples (not shown) exhibit a dominant fcc Rh(111)-Bragg peak and weaker peaks from higher-indexed Rh planes. However, the Rh peaks were found to be shifted slightly to higher Bragg angles upon increase of t_{Fe} , implying a fcc-lattice parameter (a_0) reduction with increasing Fe-film thickness from $a_0 = 3.808$ Å (pure Rh film) to 3.793, 3.780, 3.738, and 3.713 Å for t_{Fe} =2, 5, 10, and 15 Å, respectively. No pure bcc-Fe Bragg peaks could be detected. However, a shoulder (near $2\theta \approx 40^{\circ}$) on the low-angle side of the Rh(111) peak observed for the thicker Fe films (10 and 15 Å) may be assigned to a bcc (110) reflex with a corresponding bcc-lattice parameter which is enhanced (relative to that of pure bcc Fe) by 11.4% (for $t_{\rm Fe} = 10$ Å) and 10.0% (for $t_{\rm Fe} = 15$ Å). In view of the small-angle XRD and Mössbauer results (below) the observed reduction or increase in lattice parameter is interpreted by the main effect of interface-fcc-alloy formation or bcc-alloy formation, respectively. For fcc Fe-Rh alloys, our interpretation is qualitatively supported by the known decrease of a_0 with rising Fe content in the bulk.³

Mössbauer spectra measured at 4.2 K (Fig. 2) indicate magnetic hyperfine (hf) splitting at all Fe thicknesses. These spectra were least-squares fitted using a histogram distribution, 4 $P(B_{\rm hf})$, of hyperfine fields $B_{\rm hf}$. It was found necessary to include a small linear correlation between isomer shift δ and $B_{\rm hf}$, given by about +0.004 mm s⁻¹/T.

For $t_{\rm Fe}$ =2 Å, the most-probable (peak) hf field, $B_{\rm hf}^{\rm peak}$, has a value of 16.8 T (Fig. 2) which is typical for that of a ~7 at. % Fe disordered fcc-Fe-Rh bulk alloy at 4.2 K.⁵ This

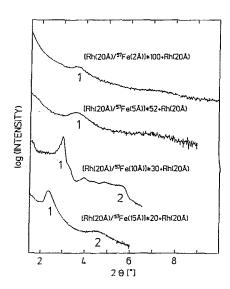


FIG. 1. Small-angle XRD patterns of Rh(20 Å)/ 57 Fe($t_{\rm Fe}$) multilayers with $t_{\rm Fe}$ =2, 5, 10, and 15 Å (from top) (Cu $K\alpha$ radiation).

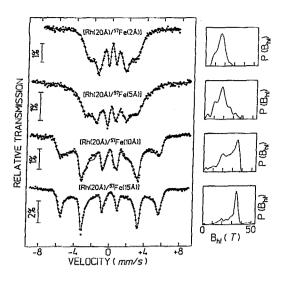


FIG. 2. Mössbauer spectra measured at 4.2 K and distributions $P(B_{\rm hf})$ of Rh(20 Å)/ 57 Fe($t_{\rm Fe}$) multilayers for $t_{\rm Fe}$ =2, 5, 10, and 15 Å (from top).

suggests that the 2 Å ⁵⁷Fe film [~1 monolayer (ML) bcc Fe(110)] is completely alloyed with Rh resulting in an fcc-Fe-Rh alloy of average Fe concentration $c_{\rm Fe}^{B_{\rm hf}}$ of \sim 7 at. %. In the case of $t_{\rm Fe}$ =5 Å, $P(B_{\rm hf})$ in Fig. 2 shows a pronounced peak at 18.2 T which demonstrates that this is also a pure fcc-RhFe multilayer. This hf field corresponds to $c_{\rm Fe}^{B_{
m hf}}$ ~ 19 at. %, according to Ref. 5. We have also estimated the Fe concentration $(c_{Fe}^{a_0})$ in the fcc-alloy layer by comparing the measured lattice parameters (a_0) with those of bulk alloys.³ Table I shows that $c_{\rm Fe}^{a_0}$ values for 2 and 5 Å Fe are in rough agreement with corresponding $c_{\text{Fe}}^{B_{\text{hf}}}$ values. The calculated Rh thicknesses, $t_{\text{Rh}}^{\text{fcc}}$ alloy, required for explaining the obtained $c_{\text{Fe}}^{B_{\text{hf}}}$ or $c_{\text{Fe}}^{a_0}$ values are given in Table I, too. (It was assumed that $t_{\rm Fe}$ =2 and 5 Å are completely alloyed). The $t_{\rm Rh}^{\rm fcc}$ alloy values obtained from $c_{\rm Fe}^{B_{\rm hf}}$ appear somewhat too large as compared to the deposited 20 Å-Rh layer, while those values deduced from $c_{\rm Fe}^{a_0}$ appear to be reasonable. Table I indicates also the Fe concentration $(c_{Fe}^{T_f})$ obtained by com-

TABLE I. Estimated Fe concentrations $c_{\rm Fe}^{T_f}$, $c_{\rm Fe}^{B_{\rm hf}}$ and $c_{\rm Fe}^{a_0}$ of the fcc and bcc Rh-Fe alloy phase in Rh/Fe multilayers. $t_{\rm Rh}^{\rm fcc}$ alloy is the calculated Rh thickness consumed in fcc-alloy formation.

Rh(20 Å)/Fe(t _{Fc})	$t_{\rm Fe}$ =2 Å	$t_{\rm Fe}$ =5 Å	$t_{\rm Fe} = 10 \text{ Å}$	$t_{\rm Fe}$ =15 Å
fcc phase				
$c_{\rm Fe}^{T_f}$ /at. %	7	12	24	•••
(t fcc alloy)	(25 Å?)	(34 Å?)	(9.4 Å?)	•••
$c_{\rm Fe}^{B_{ m hf}}$ /at. %	~7	~19	>25	>25
$(t_{Rh}^{f\infty alloy})$	(25 Å?)	(20 Å?)	•••	•••
c #0/at. %	10	24	50	62
(troc alloy)	(17 Å)	(14.8 Å)	(3.0 Å)	(1.2 Å)
bcc phase				
$c_{ m Fe}^{B_{ m hf}}$ /at. %	•••	•••	~96	~96

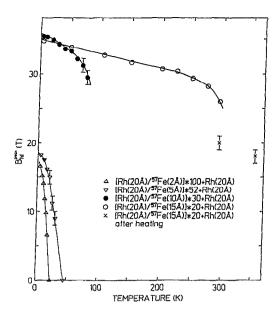


FIG. 3. Temperature dependence of $B_{\rm F}^{\rm eak}$ for $t_{\rm Fe}{=}2~{\rm \AA}~(\triangle)$, 5 ${\rm \AA}~(\nabla)$, 10 ${\rm \AA}~(\bigoplus)$ and 15 ${\rm \AA}~(\bigcirc)$. Crosses (×): for $t_{\rm Fe}{=}15~{\rm \AA}$ after annealing at 355 K.

paring the measured (average) magnetic transition temperature T_f of our films ($T_f{=}23{\pm}4~\rm K$ for $t_{\rm Fe}{=}2~\rm \mathring{A}$ and $T_f{=}45{\pm}7~\rm K$ for $t_{\rm Fe}{=}5~\rm \mathring{A}$, respectively, see Fig. 3) with the T_f vs $c_{\rm Fe}$ behavior of disordered fcc-RhFe alloys; however, the corresponding (calculated) $t_{\rm Rh}^{\rm fcc}$ alloy values (Table I) are unreasonably high (e.g., 34 $\rm \mathring{A}$ for $t_{\rm Fe}{=}5~\rm \mathring{A}$). This very likely indicates that the T_f vs $c_{\rm Fe}$ behavior in ultrathin RhFe alloy layers deviates from that in bulk alloys as is the case for other spin glasses. From the Mössbauer-line-intensity ratios the Fe-spin orientation in these samples was found to be nearly random which can be expected for spin-glass-type magnetism where a magnetic shape anisotropy is absent.

One can notice in Fig. 2 that the $P(B_{\rm hf})$ curves (and the spectra) change drastically with increasing Fe thickness: the fcc-alloy distribution peak near ~17 T decreases gradually in relative intensity and shifts to slightly higher values, while simultaneously a new peak near 36 T (35 T) evolves and dominates at $t_{\rm Fe}$ =10 Å (or $t_{\rm Fe}$ =15 Å). This new peak is assigned to a disordered ferromagnetic bcc-Fe-Rh alloy. This follows from a comparison of our $B_{\rm hf}^{\rm beak}$ values with those of Fe-rich disordered bcc-Fe-Rh bulk alloys. We may estimate the average composition $c_{\rm Fe}$ of the bcc alloy in our multilayers by using the $B_{\rm hf}$ vs $c_{\rm Fe}$ curve in Ref. 7 (with $B_{\rm hf}$ in Ref. 7 corrected by a factor of 1.03 for the low temperature (4.2 K) used in our case). This leads to $c_{\rm Fe}$ ~96 at. % for $t_{\rm Fe}$ =10 and 15 Å in the bcc alloy (Table I).

The shape of the distribution $P(B_{\rm hf})$ for $t_{\rm Fe}=10$ Å (Fig. 2) demonstrates that fcc and bcc alloy phases coexist in this multilayer, (with the fcc-alloy distribution peak located at 19.8 T). Even for $t_{\rm Fe}=15$ Å, the fcc-alloy distribution peak (at 20.0 T) is still present, together with a low-field distribution part (for $B_{\rm hf}<28$ T). The relative area of the low-field or high-field ($B_{\rm hf}>28$ T) distribution part provides values for the relative phase content (fcc or bcc) in the multilayer. In the case of $t_{\rm Fe}=10$ Å we find that (36±15)% of the Fe atoms form the fcc-interface alloy (and 64% the bcc phase); for

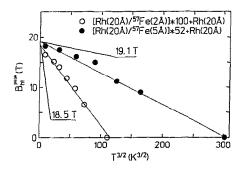


FIG. 4. B_{hf}^{peak} vs $T^{3/2}$ for $t_{Fe}=2$ Å (O) and 5 Å (\blacksquare).

 $t_{\rm Fe}$ =15 Å, the corresponding values are (30±5)% (fcc) and 70% (bcc). This means that in the average a thickness of 3.6 Å Fe of the original 10 Å bcc-Fe layer is transformed to the fcc-interface alloy by interdiffusion; for the 15 Å Fe film, the corresponding value is 4.5 Å Fe. The Fe-spin direction of the bcc phase was observed to be preferentially oriented in the film plane indicating a shape anisotropy due to ferromagnetism.

It follows from the temperature dependence of B_{hf}^{peak} (Fig. 3) that the magnetic transition temperatures of the bcc phase (in multilayers with $t_{Fe}=10$ and 15 Å) are much higher than those of the fcc phase (with $t_{\rm Fe}=2$ and 5 Å). For $t_{\rm Fe}=2$ and 5 Å, $B_{\rm hf}^{\rm peak}(T)$ follows closely a $T^{3/2}$ -spin wave law over the whole temperature range (Fig. 4). For $t_{\rm Fe}=15$ Å, $B_{\rm hf}^{\rm peak}$ shows a remarkable linear T dependence over a wide T range. It has been suggested that such a behavior is related to superparamagnetic relaxation of bcc-phase clusters.8 However, as we have not observed a remarkable change at 150 K in the central component of the spectrum (not shown) even by applying fields up to 1 T, we may exclude superparamagnetism. Therefore, the linear T dependence observed can be explained by quasi-two-dimensional behavior of the bcc phase in the 15-Å sample, as predicted theoretically.9 In contrast, the $t_{\rm Fe}=10$ Å multilayer has been observed to be superparamagnetic by applying a magnetic field. After a measurement at 355 K and recooling to 295 K, an irreversible drop of $B_{\rm hf}^{\rm peak}$ at 295 K occured. As we did not observe a change in $P(B_{hf})$ at 4.2 K after annealing, this drop in B_{hf}^{peak}

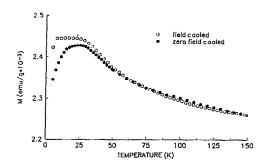


FIG. 5. Temperature dependence of magnetization in a Rh(20 Å)/ 57 Fe(2 Å) multilayer measured in $B_{\rm ext}$ =0.5 T, zero-field cooled (\odot) and field cooled (\bigcirc).

could be due to a change in bcc Fe-film morphology (island formation) and a resulting change in the T dependence of $B_{\rm hf}^{\rm peak}$ (possibly due to superparamagnetism).

The temperature dependence of the magnetization in the multilayer with $t_{\rm Fe}{=}2$ Å (Fig. 5) indicates typical spin-glasslike behavior, i.e., different branches after zero-field cooling and during field cooling. It can be seen that the temperature of the maximum in the zero-field cooled magnetization (23 \pm 2 K) is in very good agreement with the magnetic transition temperature obtained from Mössbauer spectroscopy. This proves that interface fcc alloys with spin-glasslike properties can be obtained in Rh/Fe multilayers.

We are grateful to U. von Hörsten for technical assistance and sample preparation. This work was supported by the DFG (SFB166).

¹ For an overview of recent work, see Proceedings of the First International Symposium on Metallic Multilayers, Kyoto, Japan, 1993 [J. Magn. Magn. Mater 126 (1993)].

²O. Kubaschewski, *Iron Binary Phase Diagrams* (Springer, Berlin, 1992).

³C. C. Chao, P. Duwez, and C. C. Tsuei, J. Appl. Phys. 42, 4282 (1971).

⁴J. Hesse and A. Rübartsch, J. Phys. E 7, 526 (1974).

 ⁶ B. Window, G. Longworth, and C. E. Johnson, J. Phys. C 3, 2156 (1970).
 ⁶ H. Vloeberghs *et al.*, Europhys. Lett. 12, 557 (1990).

⁷G. Shirane, C. W. Chen, P. A. Flinn, and R. Nathans, J. Appl. Phys. 34, 1044 (1963).

⁸ Z. Q. Qiu, S. H. Mayer, C. J. Gutierrez, H. Tang, and J. C. Walker, Phys. Rev. Lett. 63, 1649 (1989).

⁹J. C. Levy and J. L. Motchane, J. Vac. Sci. Technol. 9, 721 (1971); J. A. Davis, J. Appl. Phys. 36, 3520 (1965).